metals

MDPI

Review

Salar de Atacama Lithium and Potassium Productive Process

David Torres [1,*], Kevin Pérez [1], Felipe M. Galleguillos Madrid [2], Williams H. Leiva [3], Edelmira Gálvez [4], Eleazar Salinas-Rodríguez [5], Sandra Gallegos [1], Ingrid Jamett [6,7], Jonathan Castillo [8], Manuel Saldana [1] and Norman Toro [1,*]

1 Faculty of Engineering and Architecture, Universidad Arturo Prat, Iquique 1110939, Chile; kevin.perez@sqm.com (K.P.); chichined@gmail.com (S.G.); masaldana@unap.cl (M.S.)
2 Centro de Desarrollo Energético Antofagasta, Universidad de Antofagasta, Antofagasta 1240000, Chile; felipe.galleguillos@uantof.cl
3 Facultad de Ingeniería, Arquitectura y Diseño, Universidad San Sebastián, Concepción 4030000, Chile; williams.leiva@uss.cl
4 Departamento de Ingeniería Metalúrgica y Minas, Universidad Católica del Norte, Antofagasta 1270709, Chile; egalvez@ucn.cl
5 Academic Area of Earth Sciences and Materials, Institute of Basic Sciences and Engineering, Autonomous University of the State of Hidalgo, Pachuca 42184, Mexico; salinasr@uaeh.edu.mx
6 Centro de Economía Circular en Procesos Industriales (CECPI), Facultad de Ingeniería, Universidad de Antofagasta, Antofagasta 1270300, Chile; ingrid.jamett@uantof.cl
7 Departamento de Ingeniería Industrial, Facultad de Ingeniería, Universidad de Antofagasta, Antofagasta 1240000, Chile
8 Departamento de Ingeniería en Metalurgia, Universidad de Atacama, Copiapó 1531772, Chile; jonathan.castillo@uda.cl
* Correspondence: dtorres.albornoz@gmail.com (D.T.); notoro@unap.cl (N.T.); Tel.: +56-975387250 (N.T.)

Abstract: The average lithium content in the Earth's crust is estimated at about 0.007%. Despite this, lithium is considered abundant and widely distributed, with significant extraction from various sources. Notably, the brines in the Salar de Atacama are highlighted for their high lithium concentration ~1800 mg/L. Lithium is currently recovered from these brines through a solar evaporation process. The brine is transferred through a series of ponds, increasing the lithium concentration from 0.2% to 6% over 18 months, while decanting other minerals like potassium, magnesium, and boron. This method is the most efficient and cost-effective globally due to the Salar de Atacama's high lithium concentration of approximately 1800 ppm and the region's intense solar radiation, which facilitates evaporation at no economic cost. This manuscript describes in detail the lithium and potassium extraction processes used in the Salar de Atacama.

Keywords: brines; solar evaporation; lithium carbonate; lithium hydroxide

Citation: Torres, D.; Pérez, K.; Galleguillos Madrid, F.M.; Leiva, W.H.; Gálvez, E.; Salinas-Rodríguez, E.; Gallegos, S.; Jamett, I.; Castillo, J.; Saldana, M.; et al. Salar de Atacama Lithium and Potassium Productive Process. *Metals* **2024**, *14*, 1095. https://doi.org/10.3390/met14101095

Academic Editors: Mohamad El Mehtedi and Mauro Carta

Received: 16 August 2024
Revised: 12 September 2024
Accepted: 17 September 2024
Published: 24 September 2024

1. Theoretical Lithium Background

1.1. Lithium Deposits—Introduction

The average lithium content in the Earth's crust is estimated at about 0.007% [1]. Despite this, lithium is considered to be an abundant and widely distributed metal. It can be extracted from various sources, including brines, pegmatites, and sedimentary rocks. Brine deposits are further classified into continental brines, geothermal brines, and oil field brines [2].

Among these sources, continental brines and pegmatites (hard rock ore) are the primary contributors to commercial lithium production. While estimates of lithium resources and reserves vary, it is generally agreed that brine resources are significantly more abundant than those found in hard rock [3].

1.2. Lithium Deposits in Continental Brines

Although lithium is considered abundant in nature, only very specific regions in the world contain lithium-enriched brine deposits. Most of the commercially exploited brine deposits are found in endorheic basins, where concentration by evaporation is favored [3].

It is estimated that about 66% of the world's lithium resources are housed in South American continental brines in the so-called Lithium Triangle, which includes deposits in Bolivia, Chile, and Argentina (Figure 1). There are also inland brine resources in the southeastern United States, Australia, Israel, China, and Tibet. The most extraordinary example is the Salar de Atacama in Chile, with its nearly 3000 km^2, it has an average lithium concentration of 0.14%, the highest known, with resources estimated at 9.1 million tons, which allows the production of more than 45 million tons of equivalent lithium carbonate. Albemarle's Silver Peak lithium mine in Nevada is the only lithium operation from inland brines in the United States [4].

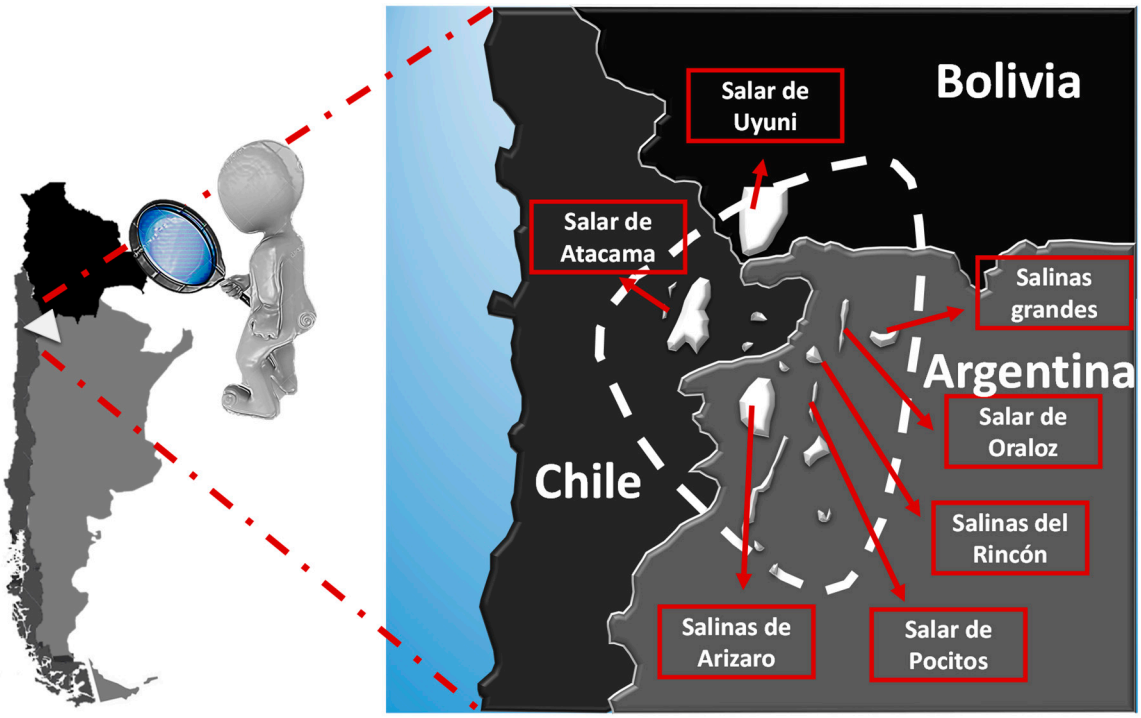

Figure 1. Lithium Triangle.

2. Lithium Production Process in Continental Brines

2.1. Fractional Precipitation

Fractional precipitation for lithium production from continental brines broadly follows the same processing methodology, even though the nature of the brine differs between different salt flats around the world [5]; however, it stands to reason that this process has its particularities depending on the composition of the brine; therefore, the evaporation process must be adapted to each case to maximize yields.

Even though the concentration of lithium in continental brines is the highest compared to geothermal and petroleum sources, its content is still too low for the direct production of lithium carbonate or lithium hydroxide. Normally, exploited brine deposits do not exceed a few hundred parts per million (ppm) and added to the presence of impurities in the brine [6], the dominant methodology for the production of high purity lithium begins with the solar evaporation that is based on the fractional precipitation and with it an increase in the concentration of lithium in the brine. In this process, the crystallization of salts occurs in solar evaporation ponds, which are shallow and have extensive surfaces exposed to

solar radiation [7], where the objective is to obtain a concentrated brine of lithium in a sustainable way and at a low cost, reaching contents around 6000 mg/L.

2.2. Solubility

Electrolytes are substances that are characterized because they dissociate into free ions by the simple fact of their aqueous solution. These may already be pre-formed in the solid, as is the case with ionic substances, such as sodium chloride, potassium chloride, magnesium chloride, and lithium chloride. There are ionic substances that do not dissolve completely in water, thus obtaining a saturated solution of ions in the presence of a solid. This is the typical case of fractioned precipitation in solar evaporation ponds.

Solubility is the measure of the ability to dissolve a certain substance in a certain medium, and under specific conditions of temperature and pressure. During this process of evaporation and concentration, the brine, increasingly saturated in low solubility salts, generates the precipitation of chlorides and/or sulfates depending on the nature of the brine. The order or sequence of precipitation is controlled by the differential solubility of the different salts. Solubility is the most important parameter in fractional precipitation processes, establishing itself as the greatest driving force to separate. Table 1 shows the solubility of different chlorides at 25 °C.

Table 1. Solubility of chloride salts at 25 °C (Modified from: [4]).

Compound	Solubility (g/100 gH_2O)
LiCl	84.5
$CaCl_2$	81.3
$MgCl_2$	56.0
KCl	35.5
NaCl	36.0

According to the fractional precipitation processes in chloride brines, the less soluble salts are the first to precipitate in the ponds, and this is manifested through the crystallization of sodium chloride and potassium chloride, with a solubility of 36.0 g/100 mL and 35.5 g/100 mL, respectively.

The solubility of lithium chloride in water is more than double with respect to sodium chloride or potassium chloride; it is for this reason that in the most diluted ponds of the Salar de Atacama, the precipitation of salts associated with lithium does not generate, for example, lithium carnallite. If the concept of solubility is not fully understood, it is not possible to know or control the processes that occur in solar evaporation ponds [3,4,8].

2.3. Common Ion Effect

The solubility indicators presented previously in Table 1 occur under an ideal scenario; that is, there is no interaction with other ions, such as calcium, magnesium, sulfates, or other chlorides. In practical terms, only one solute is present at a time. But what happens when solutions with two solutes containing the same ion are present? This is the scenario where the so-called common ion appears, which may well be a cation or an anion.

The solubility of a salt changes if other substances that provide common ions are added to the solution. As an example, we consider the addition of NaCl on the solubility of KCl, where sodium chloride has a significant effect on the solubility of KCl due to the addition of chloride ions. The solubility constant is expressed as a function of the ion concentrations and the mean activity coefficient of the ions ($\gamma_{\pm}$) in the saturated solution [9].

The following ionic equations describe the process of the common ion effect.

$$K^{+}_{(aq)} + Cl^{-}_{(aq)} = KCl_{(s)} \quad (1)$$

$$NaCl_{(s)} = Na^{+}_{(ac)} + Cl^{-}_{(ac)} \quad (2)$$

$$NaCl_{(s)} + K^{+}_{(aq)} + Cl^{-}_{(aq)} = KCl_{(s)} + Na^{+}_{(aq)} + Cl^{-}_{(aq)} \quad (3)$$

The chloride ion concentration will increase and therefore the K^+ ion concentration will have to decrease to keep the K_{ps} constant, thus decreasing the solubility of KCl.

$$K_{ps} = C^{+}_{K} \times C^{-}_{Cl} \times \gamma^{2}_{\pm} \quad (4)$$

Figure 2 shows the decrease in the KCl concentration as the sodium chloride concentration increases.

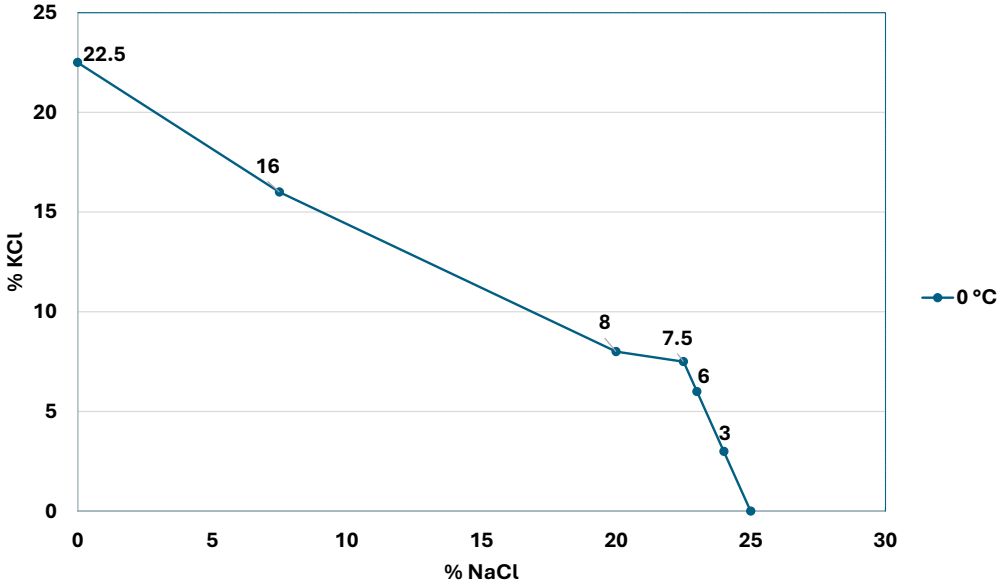

Figure 2. Solubility curve of sodium and potassium chloride at 0 °C (modified from: [4]).

In the case of the lithium chloride generating systems of the Salar de Atacama, the common ion is chloride; in all the ponds, sodium chloride precipitates and the chloride concentration in the brine will increase. In this case, the solubility curve behaves like a parabola, as described by Equation (4) [9].

2.4. Operational Parameters

In addition to the lithium content, in the design of the evaporation process, other parameters associated with the elements present in the brine must be considered, which are detailed below:

- **Mg/Li ratio:** Determines the amount of magnesium that must be removed by fractional crystallization or selective precipitation. Currently, mainly brines with low Mg/Li ratios are used for lithium production [10], while a Mg/Li ratio greater than 10 has not made production on an industrial scale profitable. Magnesium is particularly difficult to separate from lithium, in part, because they are elements with very similar properties. There is a diagonal relationship between the two, this mainly because the atomic and ionic sizes are similar [11]. Li^+ has a radius of 0.60 °A (0.06 nm) and Mg^{2+} a radius of 0.65 °A (0.065 nm). For its part, Na^+ has a radius of 0.95 °A (0.095 nm), which makes it almost incompatible to replace lithium or magnesium in a crystalline structure (See Figure 3). This is evident when lithium carbonate presents properties similar to magnesium carbonate and not to the homologues of its group such as potassium carbonate or sodium carbonate [12]. In many other respects, lithium resembles magnesium and other alkaline earth elements and differs from the properties of Group 1 alkali metals. Diagonal relationships are important to predict the chemical behavior of a given element, as well as its compounds [13].

- **SO_4/Li Ratio:** This parameter determines if the deposit is lithium chloride (low SO_4/Li) or lithium sulfate (high SO_4/Li). At a high ratio, lithium sulfate salts typically begin to precipitate from lithium concentrations between 0.5% and 1% [14]. The determination of the type of deposit can alternatively be identified through the **SO_4/Mg ratio** (see Table 2).
- **Ca/Li ratio:** Determines the amount of calcium that must be removed by fractional crystallization or selective precipitation.
- **SO_4/K Ratio:** Indicates a Potassium Sulfate deposit (high SO_4/K) or Potassium Chloride deposit (low SO_4/K).
- **SO_4/Ca ratio**: When calcium concentrations are high, sulfate concentrations are low, and the same thing happens inversely. This parameter also defines yield losses due to lithium sulfate precipitation when sulfate contents are in excess, that is, with a SO_4/Ca ratio greater than 2.4, which represents the stoichiometric ratio for calcium sulfate precipitation. Values above 2.4 can cause lithium sulfate precipitation in more concentrated systems. For this reason, it is said that calcium is a regulator of sulfate content. In this sense, this is one of the most relevant parameters for the definition of fractional precipitation processes [4].

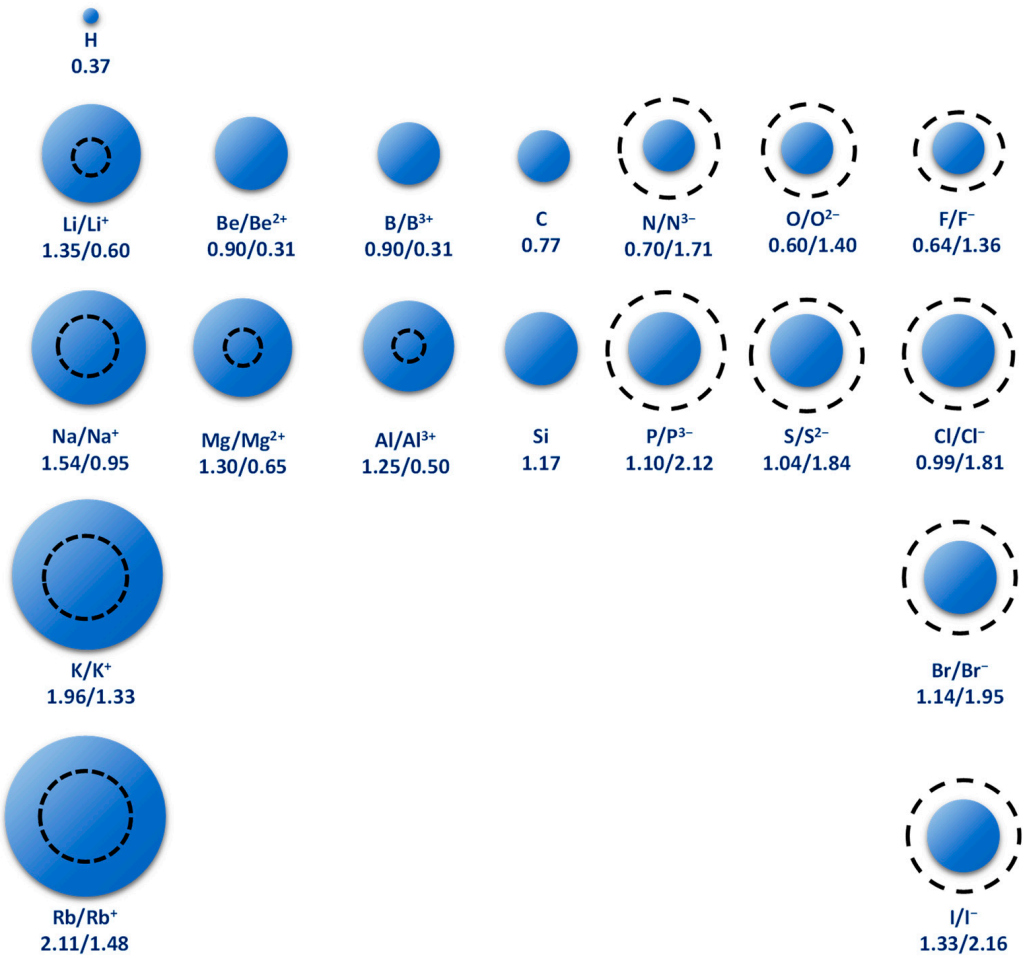

Figure 3. Relative atomic radii of some elements compared to the atomic radius of ions. The atomic radius is expressed in units of Å. The solid sphere represents atoms and the dashed circle represents ions (modified from: [4]).

Table 2. Chemical composition and relationship of elements in different continental brine deposits (modified from: [4]).

Deposit Characteristics (mg/L)									
Deposit	**Li**	**K**	**Mg**	**Ca**	**SO_4**	**B**	**Mg/Li**	**SiO_4/Li**	**Ca/Li**
Salar de Atacama Average	1835	22,626	11,741	379	20,000	783	6.4	10.9	0.2
Salinas Grandes Salt Flats	775	9289	2117	1450	1036	232	2.7	1.3	1.9
Dead Man's Salt	744	7404	1020	636	10,236	420	1.4	13.8	0.9
Salar de Hombre Muerto EastSide	745	8318	1781		8642		2.4	11.6	
Silver Peak	245	5655	352	213	7576	85	1.4	30.9	0.9
Salar de Olaroz (production Wells)	774	6227	2005	416	18,630	1136	2.6	24.1	0.5
Cauchari Salt Flat	618	5127	1770	476	19,110	1360	2.9	30.9	0.8
Salar de Uyuni Average	424	8719	7872	557	10,342	2442	18.6	24.4	1.3
Rincon Salt Flats	397	7513	3419	494	12,209	331	8.6	30.7	1.2
Maricunga Salt Flat	1036	8869	8247	11,919	1095	634	8.0	1.1	11.5

In the case of the chloride brines of the Salar de Atacama, with a medium–high Mg/Li ratio, gypsum precipitation occurs ($CaSO_4 \times 2H_2O$) and halite (NaCl) precipitation occurs in the first ponds. As the brine is concentrated in these systems, other simple salts such as sylvite (KCl) and bischofite ($MgCl_2 \times 6H_2O$) or double salts such as sylvinite (KCl × NaCl) and potassium carnallite (KCl $MgCl_2 \times 6H_2O$). More sulfated systems such as Silver Peak or Olaroz require a liming treatment, where a significant part of the magnesium is removed [15,16]

During the evaporation process, a brine is obtained that contains a progressively higher concentration of the most soluble components, such as lithium and boron, compared to other ions such as potassium and sodium, which have decreased their content. in the most concentrated systems at the end of the evaporation process [17]. In addition to magnesium, boron, potassium, and sodium, this brine has low calcium and sulfate contents, which must be removed anyway before conversion to lithium carbonate.

On the other hand, the salts sequentially precipitated in the ponds are harvested and accumulated in piles for their final disposal or they can be derived to different processes to obtain other products or by-products, such as potassium chloride, boric acid, or potassium sulfate, among others.

The main drawbacks of lithium production from continental brines are concentrated in the long operating times of the evaporation systems, which are normally greater than 12 months. The evaporation rate is controlled by solar radiation, ambient temperature, water content, wind, and precipitation rate. In general, solar evaporation has an approximate recovery of 50% [18]. Losses are generated by undesired precipitation of lithium salts, brine filtration into the subsoil, and/or impregnation of lithium brine into the precipitated salts. The presence of impurities such as magnesium and sulfate can make the process unfeasible.

To avoid losses due to filtration (also called infiltration), the construction of the ponds must comply with the conditions that allow brine to be retained, preventing infiltration into the subsoil. For this purpose, the ponds are usually waterproofed with a high-density geotextile joined by thermofusion. In the ponds of the Salar de Atacama in Chile and northern Argentina, a layer of halite approximately 30 cm high is usually additionally present, which has been collected from the harvests of the first ponds in the fractional precipitation process. This layer of halite protects the impermeable base during the salt harvest periods, when the traffic of heavy machinery demands the impermeable floor to the maximum [19].

On the other hand, undesired lithium precipitation occurs due to the presence of impurities such as sulfate, which in excess generates the crystallization of lithium sulfate. Magnesium in turn precipitates lithium as lithium carnallite (LiCl $MgCl_2 \times 7H_2O$), which is why its contents must be controlled.

Losses due to impregnation are associated with the mechanical dragging of the brine in the crystallized salts at the base of the ponds. To control these losses, good drainage must be ensured during the drying stage of the ponds, as well as efficient collection of the

drained brine. In the Salar de Atacama, stages of leaching or washing of salts impregnated with lithium have been incorporated, significantly improving the yields of the process [4].

2.5. Conversion to Lithium Carbonate and Lithium Hydroxide

In the previous stage, the concentration process by fractional precipitation was explained, where the product corresponds to a brine with lithium concentrations that can vary between 4% and 6%. The impurities associated with boron, magnesium, calcium, sulfate, sodium, and potassium must be removed before carbonation of lithium chloride [3].

Magnesium is usually removed with the addition of a base (usually slaked lime) to precipitate magnesium hydroxide. Other monovalent cations remain in solution due to the difference in solubility of their hydroxide, shown in Table 3.

Table 3. Solubility of hydroxide salts at 25 °C (Modified from: [4]).

Compound	Solubility [g/100 g H_2O)
LiOH	12.5
NaOH	100
KOH	120.8
$Mg(OH)_2$	0.00069

Lithium carbonate is finally precipitated by adding sodium carbonate Na_2CO_3 and then dried. Since magnesium and calcium are removed beforehand, only lithium precipitates as lithium carbonate. Some sodium and potassium ions remain in solution, but these species can be ignored due to the difference in solubility of their carbonate salts, as shown in Table 4. This lithium carbonate is itself a product and can be a source from other lithium compounds such as lithium hydroxide LiOH [20].

Table 4. Solubility of carbonate salts at 25 °C (modified from: [4]).

Compound	Solubility [g/100 g H_2O)
Li_2CO_3	1.3
$NaCO_3$	30.7
K_2CO_3	111.4
$MgCO_3$	0.18
$CaCO_3$	0.00066

3. The Salar de Atacama

The Salar de Atacama, with an area of 3000 km^2, is the largest in Chile [21]. It is located in an endorheic basin limited by two morphostructural strips of regional scale.

To the west it borders the Cordillera de la Sal, whose peaks reach a few hundred meters above the level of the salt flat. It extends for almost 80 km in a north-northeast to south-southwest direction at the foot of the Domeyko Mountain Range. To the east, the basin is limited by the Andes Mountains. The Cordón de Lila, characterized by the outcropping of rocks, forms a unique morphotectonic feature in the region, and marks the southern limit of the evaporitic deposits that make up the Salar de Atacama (SQM Online). As a consequence of tectonics and an arid climate, the Salar de Atacama is a closed or endorheic basin [22], which covers an area of more than 18,000 km^2 (see Table 5).

The Marginal Zone and the Nucleus are present in the Salar de Atacama [23], which make up two well-defined hydrogeological units. These units have various resources, such as important aquifers, unique flora, and fauna ecosystems, as well as large reserves of potassium and lithium minerals, which, in this natural brine subsystem, represents the main source for lithium production in Chile [24]. On the other hand, the highest lithium concentrations have been reported in the Salar de Atacama than in any other continental brine system in the world (see Table 6). These lithium enrichment zones are

concentrated around the Salar Fault System (SFS), with average contents in the basin around 1400 mg/L [25].

Table 5. Main morphometric and climatological characteristics (modified from: [22]).

Height (m)	2300
Basin Surface (km^2)	18,100
Salar surface (km^2)	3000
Surface of the lagoon (km^2)	12.6
Salar Precipitation (mm/year)	25
Mountain Range Precipitation (mm/year)	300
Salar potential evaporation (mm/year)	2000
Mountain range potential evaporation (mm/year)	1600

Table 6. Salt flats of the world and their characteristics (modified from [4]).

Basin	Region	Li Min (mg/L)	Li Max (mg/L)	Mean Li (mg/L)	Li (Mt) Resources
Atacama Salt Flats	Chile	900	7000	1800	6.3
Maricunga Salt Flat	Chile	NA	NA	920	0.22
Surire Salt Flat	Chile	NA	NA	340	8.3
Salar del Hombre Muerto	Argentina	190	900	521	0.8
Salar del Rincon	Argentina	Ma	Na	400	0.223
Salar de Olaroz and Salar de Cauchari	Argentina	282 (200 Olaroz) (250 Cauchari)	1207 (2150 Olaroz) (650 Cauchari)	650 (510 Olaroz) (450 Cauchari)	0.9–1
Llullaillaco Salt Flats (Mariana)	Argentina	250	650	450	NA
Uyuni Salt Flat	Bolivia	80	1150	321	10.2
Salar de Capaisa	Bolivia	NA	NA	243	NA
Salar de Pastos Grandes	Bolivia	353	1787	1062	NA
Clayton Valley	Nevada	100	300	160	0.3
Searles lake	California	10	80	65	NA
Salton Sea	California and Mexico	100	400	200	0.316
Great Salt Lake	Utah	18 (north) 40 (south)	43 (north) 64 (south)	52	0.53
Dead Sea	Israel	NA	NA	10	NA
Tilanier (Tainer) Lake	Qaidam, China	NA	NA	290	2.02
Dangxtongeno	Tibet, China	NA	NA	430	0.181

3.1. Marginal Zone

In this zone rich in gypsum and carbonates of approximately 1480 km^2, the main environmental protection sites are located, hosting lake ecosystems such as Los Flamencos National Reserve. The marginal zone is further subdivided into the silt zone and the efflorescence zone. The first consists mainly of clays and silts of alluvial origin, locally cemented by chlorides and sulfates. The efflorescence zone is located in a strip between the silt zone and the nucleus, and is made up of saline deposits of gypsum, anhydrite, carbonates, and borates. The marginal zone presents outcrops of a saline interface caused by the contact of fluids with different densities, such as water recharge from the Andes Mountains and high-density brine from the halite aquifer in the nucleus [26].

3.2. The Nucleus

The nucleus of the Salar de Atacama covers an area of 1400 km^2 and contains large brine reserves with high concentrations of lithium and potassium, among other elements of economic interest. The nucleus is made up of a porous structure of halite (see Figure 4) [27] and brine saturated with sodium chloride. The latter is occluded in the relatively uniform and interconnected pores of the nucleus [21]. The porosity in the nucleus decreases drastically at depths above 35 m, depending on the area evaluated. The water table in many sectors of the nucleus is approximately 1 m deep. Near the surface the porosity is around 30% [5].

Figure 4. Halite surface in the nucleus of the Salar de Atacama.

Superficially, this aquifer forms a hard and sharp crust of halite with very irregular relief because it is rarely flooded with surface water [28]. Probably, sectors of the halite nucleus have not been flooded in hundreds of years; moreover, the evaporation gradient greatly exceeds surface water inflows. Halite accumulation occurred during the Pliocene and Quaternary in conditions, alternating between a saline lake and a dry salt flat [29].

The nucleus is divided into two blocks by the Salar Fault System (SFS). In the eastern block, brines rich in SO_4 predominate, while in the western part, brines rich in Ca-Cl abound. The Li-Mg systems are concentrated in the surroundings of the Salar Fault System closest to the Cordón de Lila. The recharge of the nucleus has its origin in the recharge of surface and groundwater, in addition to the geothermal fluids of the region [30].

Among the particularities of the Salar de Atacama is not only the extraordinary lithium content, but also that it is very widespread within the halite nucleus, and is not restricted to a specific area [19]. It should be considered that lithium concentrations exceed 1000 mg/L in many sectors of the nucleus, with maximums of up to 5000 mg/L in the southern sector, near the Cordón de Lila [31].

3.3. The Origin of Lithium in the Salar de Atacama

In general, the formation of lithium brines in the world has its origin in the flows of groundwater and surface water [23,32] that converge in endorheic basins that, with the support of evaporation, concentrate solutes, leading to the precipitation of highly concentrated salts and brines. It must be considered that, unlike sodium, potassium, and calcium, lithium is highly soluble; therefore, it does not easily produce evaporites when concentrated by evaporation. On the contrary, it ends up contained in residual brines in the superficial subsoil. Different hypotheses have been described to explain the origin of lithium in the Salar de Atacama (see Figure 5); however, the extraordinary contents of this element continue to be the focus of discussion [31], given that regardless of its origin, the brine necessarily had to undergo some subsequent concentration process to bring the low lithium contents from the diluted recharge to the levels measured today in

the most enriched zone around Salar Fault Systems. Among the hypotheses, it is suggested that lithium enrichment comes from processes of weathering of volcanic rocks at low temperatures, volcanic fluids (magmatic origin), hydrothermal leaching of underground salt flats, or current filtrations in the salt flat [30].

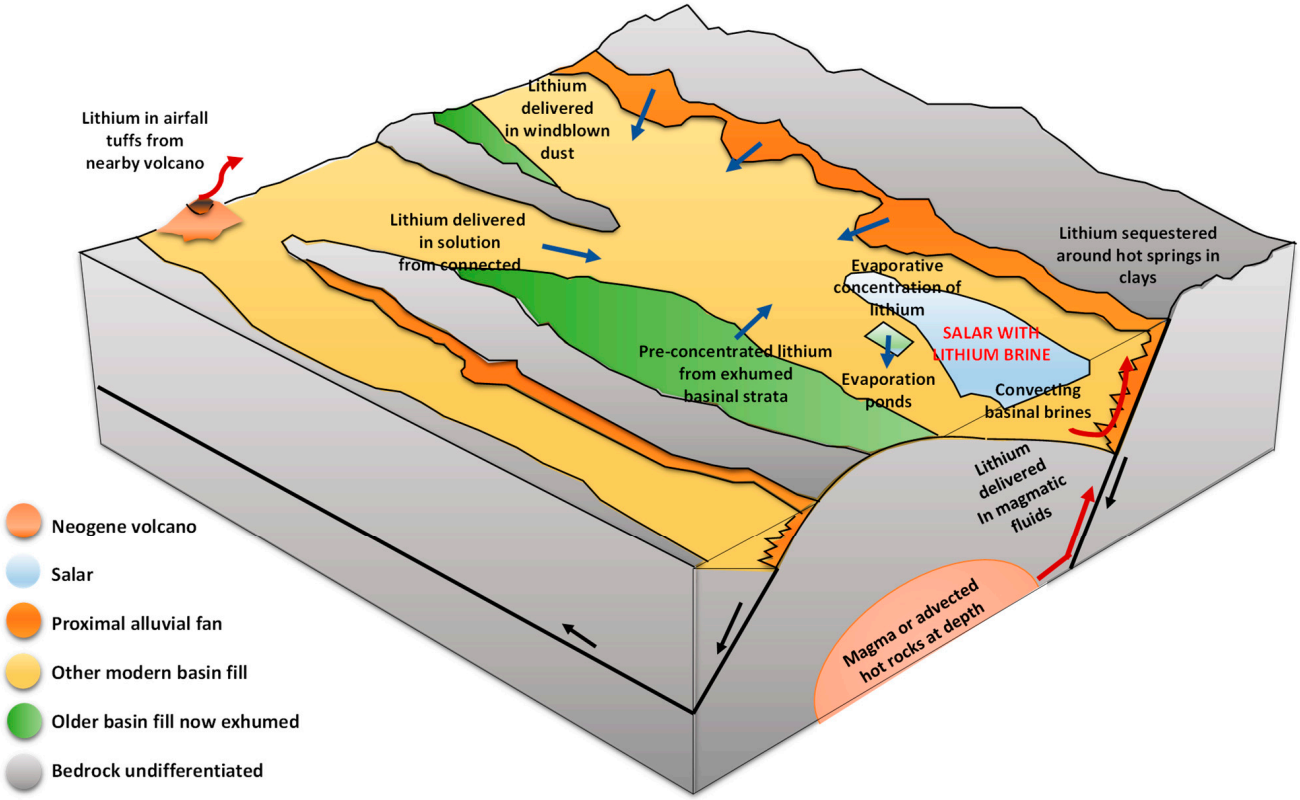

Figure 5. Origin of lithium (modified from: [4]).

Munk et al. [25] concluded that more than half of the Li in the halite nucleus originates from the eastern flank, while Jordan et al. [29] have raised the importance of the Salar Fault System (SFS), along which the rise of groundwater flows from the east take place, thus feeding the halite aquifer in the nucleus. The possibility of these groundwater flows evaporating on their way to the SFS has also been studied, thus increasing the concentrations of dissolved salts, including lithium.

Marazuela et al. [30] have suggested as a hypothesis the interaction of old layers of salts and/or clays enriched in lithium and magnesium with the diluted recharge coming from the western flank, which rapidly increases its density due to the dissolution of salts in the Cordillera de la Sal. The importance of density gradients as a driving agent of the convective displacement of diluted flows is pointed out, thus allowing the remobilization of ancient layers enriched in lithium and magnesium in the Salar fault system (SFS). Through the modeling of underground thermohaline flows in the Salar de Atacama, the author rules out a recent evaporative concentration of water recharge from the western flank as the main mechanism of lithium enrichment, due to the spatial incompatibility between lithium-rich brines and magnesium located in the SFS, and the transition sector called the minimum hydraulic head (MMH). The latter divides the Salar de Atacama basin into two isolated hydrodynamic systems where the most evaporated brines converge (see Figure 6).

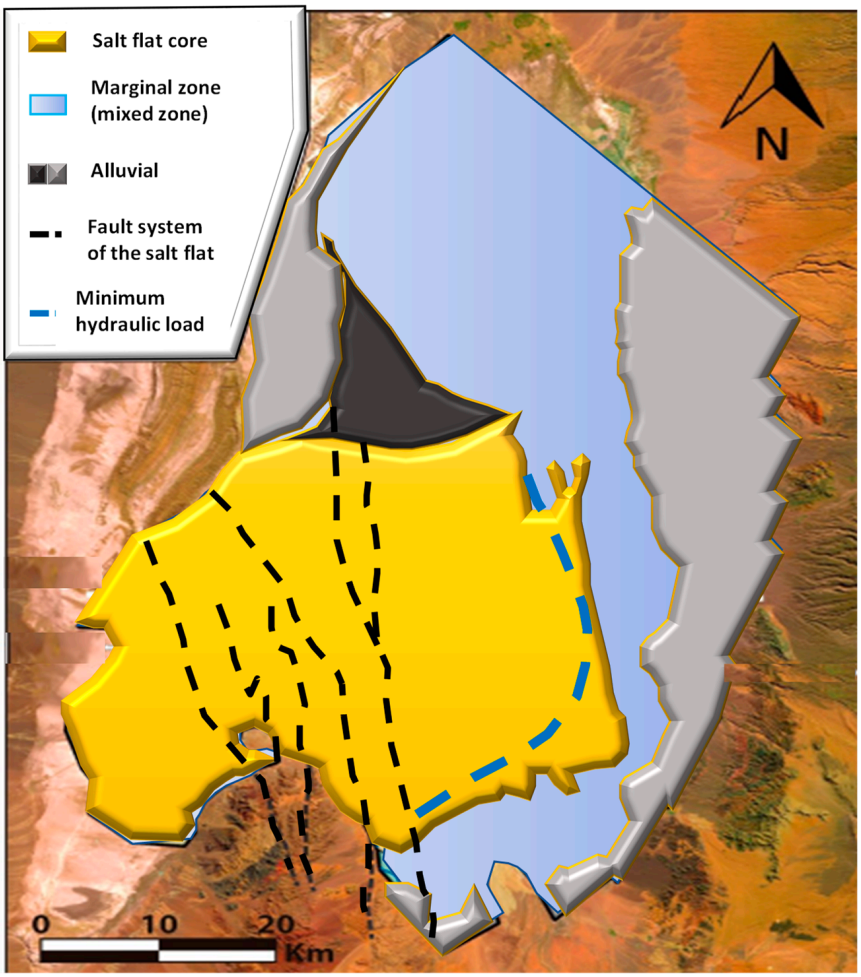

Figure 6. Hypothesis of the origin of lithium in Salar de Atacama (modified from: [4]).

4. Salar de Atacama Productive Process

4.1. Solar Evaporation Ponds

The fractional precipitation method in solar evaporation ponds is the most widely used technique for lithium recovery from brines [33]. This process has been in force for years in the operations of the Salar de Atacama, due to its low cost, lower energy consumption, and efficient management of the processes. All of this is accompanied by the extraordinary climatic conditions of the Atacama Desert, the driest place on earth, with a solar evaporation rate of 3200 mm [5], average rainfall of only 15 mm per year, and winds that favor the concentration processes of brine.

4.2. Brine Extraction

The productive process from the brines under the salt crust of the Salar de Atacama begins with the exploration and hydrogeological characterization of the nucleus, to then suck the brines through pumps at depths greater than 40 m [27] from more than 380 active wells (see Figure 7).

The brines are classified and distributed through HDPE pipes to the accumulation ponds or gutters that collect the brine from different productive wells (see Figure 8). Unlike a solar evaporation pond, these gutters can be several kilometers long and not more than 5 m wide.

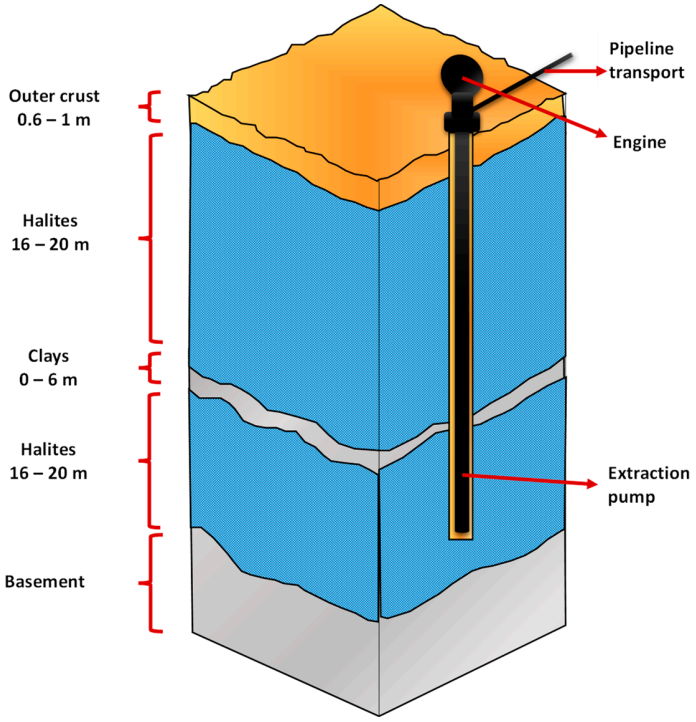

Figure 7. Porous nucleus of the Salar de Atacama and brine extraction, modified from: [4].

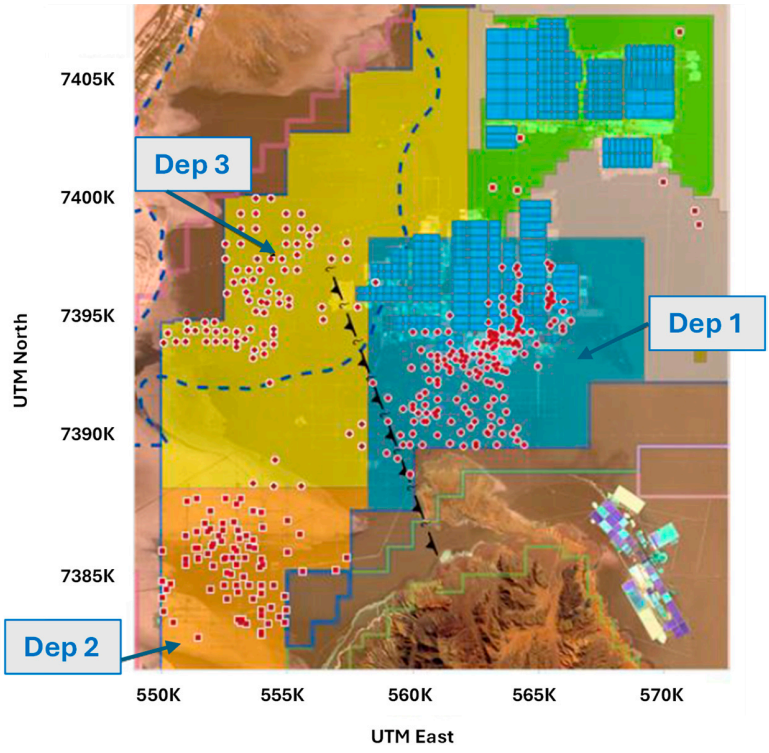

Figure 8. Productive wells in the Salar de Atacama (modified from: [4]).

Then, and by pumping, the brine is directed through pipes to the solar evaporation systems according to the projections of replenishment of ponds in the two large areas of the Salar, that is, MOPI and MOPII (see Figure 9). The first with the highest lithium and potassium contents known to date. The MOPII system presents high concentrations of sulfate and boron [34].

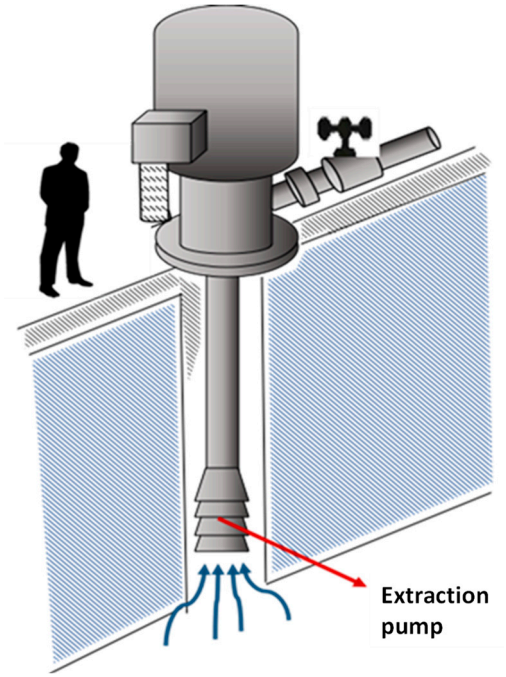

Figure 9. Brine extraction well.

The transfer volumes will be a function, among other operational parameters, of the climatic conditions, since the largest transfers are concentrated in the summer season. In this period, evaporation rates reach annual maximums.

4.3. Constructions of the Ponds

The first stage of the construction of the ponds includes the pairing of the saline crust, generating a horizontal and flat surface. As can be seen in Figure 10, the slopes of the ponds are also formed at this stage.

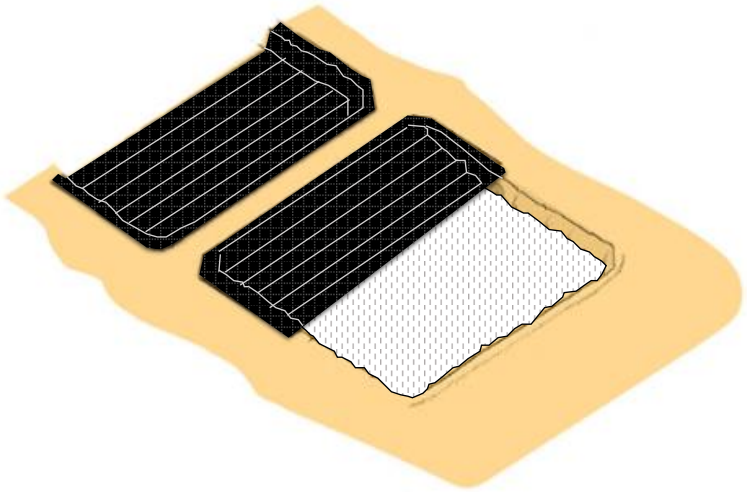

Figure 10. Construction of solar evaporation ponds.

The second stage is aimed at waterproofing the already flattened pond, as well as the slopes. For this, a layer of 300 g/m ^{2} geotextile joined by thermofusion is used, on which a 0.75 mm thick PVC waterproof membrane is placed. To waterproof the slopes, another layer of 150 g/m^2 geotextile is placed, which in turn is also covered with an HDPE membrane of 0.5 or 1 mm thickness [35]. To ensure the projected useful life of the waterproofing layers, a layer of halite salts approximately 30 cm thick is superimposed, which must be capable of

attenuating the impact caused by the transfer of heavy machinery over the pond during the salt harvest period.

In the first instance, the largest ponds that reach an area greater than 480,000 m^2 are halites. In total, the ponds cover an area of more than 42 km^2, which represents 0.5% of the surface of the Salar.

The construction of the ponds within the salt flat is carried out by breaking the saline crust and leaving a flat surface on which lies a layer of clay. The ponds are rectangular, 1.5 m deep and of various dimensions (600 × 800 m or more) and are built on the salt flat itself. Both the dikes and the bottom of the evaporation ponds are lined with a resistant plastic 0.5 mm thick. The protection of the polyurethane is achieved with a layer of NaCl salts approximately 30 cm thick.

4.4. Baffles

The interaction of brine with the winds in the Salar de Atacama have an impact on the direction of brine flows within the ponds. It is for this reason that the design of the ponds must consider their orientation with respect to the prevailing wind currents, as well as the construction of baffles that manage to efficiently distribute the grades of precipitated salts, avoiding areas of low grade due to the effect of dead volumes. This last case can occur in sylvinite systems, where due to the effect of dead zones there may be a negative impact on the potassium grade by precipitating potassium carnallite. On the other hand, the baffles serve as a series circuit within the pond, efficiently homogenizing the brine.

4.5. Pond Process

The evaporation process generates the fractional precipitation of salts in a multicomponent system depending on the degree of saturation in the brine. It is essential to know the solubility of the ions in these saline solutions for the definition of the concentration and crystallization processes. The design of the processes requires a method that allows the determination of the liquid–solid equilibrium curves in these saline systems; hence, the importance of having the appropriate thermodynamic models [36]. The thermodynamic simulation model of the crystallization process in the Salar de Atacama is based on the parameters calculated by Jerome Lukes and validated under the Pitzer model [34]. The Pitzer ionic interaction model has been widely used in the literature to represent the liquid–solid equilibrium of various aqueous electrolyte systems [24]. Figure 11 shows an aerial shot of the solar evaporation ponds in Salar de Atacama.

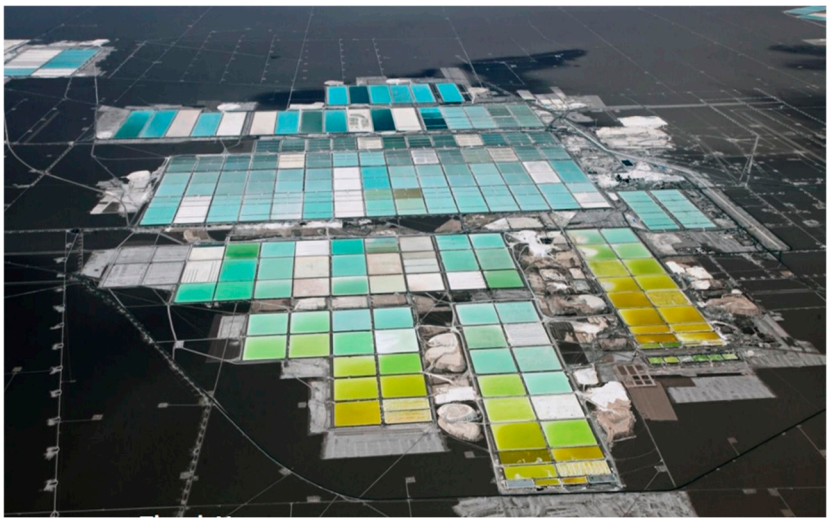

Figure 11. SQM solar evaporation ponds, Salar de Atacama (modified from: [4]).

4.6. Lithium Production Systems (MOPI)

The lithium-producing brines located in the MOPI area are characterized by having unprecedented lithium and potassium contents elsewhere on the planet, while the Mg/Li ratio is high in relation to other continental brines of the lithium triangle.

The precipitation route follows the following order: Halites–Silvinites–Potassium Carnalites–Bischofite–Lithium Carnalites. The purpose of this system is to produce sylvinite salts that meet the conditions to be fed to potassium concentrator plants and generate lithium brine for the lithium carbonate plant.

4.7. Halite Systems

Since the brine from these wells is saturated with calcium sulfate ($CaSO_4 \times 2H_2O$) and sodium chloride (NaCl), gypsum and halite are the first salts to precipitate in the wells. In these crystallization systems, halite is the main species in the precipitated salts, with a low content of gypsum and sylvite (KCl), so we are then in the halite precipitation field. Although most of the halite precipitates in these systems, its crystallization is constant throughout the process because the brine is saturated with sodium chloride at all times. The brine inputs to these systems are not saturated in potassium. At this stage, the most important thing is to precipitate the greatest amount of halite and concentrate the potassium until reaching a saturation of 95%, which should preferably precipitate in the sylvinite ponds. In these systems, magnesium acts as a tracer or indicator ion, and must be kept controlled in concentrations lower than 1.8% since, otherwise, the sylvinite precipitation field would enter, with the potassium content in the brine at around 3.5% [4]. The benefits of magnesium as an indicator of the precipitation phases are enhanced with the "ion pair curves", which plot the concentration of magnesium with respect to another ion. Changes in slope in these graphs are signs that a different salt has begun to crystallize; therefore, attention must be paid to brine transfer management between one system and another, in such a way as to avoid contamination with undesired salts in the process.

4.8. Sylvinite Systems

With the precipitation of halite and the transfer of brine to more concentrated systems, the concentration of potassium in the brine is favored and with it the precipitation field of sylvite (KCl). In this scenario, the KCl begins to progressively precipitate together with the halite in what is known as sylvinite systems (KCl + NaCl). Sylvinite salts are the raw material for the recovery of KCl in the concentrator plants of the Salar de Atacama; therefore, it is sought, as far as possible, that the halite does not precipitate in the salt-generating ponds of these plants. Potassium contents in precipitated salts in sylvinite systems can reach up to 20%, while the average feed to the concentrator plants is around 13.5%. At the end of the sylvinite ponds system, magnesium has concentrated in the brine to such an extent that the risk of potassium carnallite crystallizing increases, so it is important to keep its content in the brine under control at levels around 4.8% [3].

4.9. Potassium Carnallite Systems

Magnesium continues its concentration process in the brine until potassium carnallite ($KClMgCl_2 \times 6H_2O$) begins to precipitate when the brine is sufficiently concentrated. This characteristic makes magnesium an indicator for the control and management of brine transfers between the potassium sylvinite–carnallite systems, since it seeks to avoid its precipitation in the sylvinite systems that feed the MOP plants. When magnesium limits are defined as an indicator in process management, it is necessary to consider environmental conditions, since the balances associated with this element are sensitive to temperature changes that can be extreme in different seasons of the year. In addition to potassium carnallites, and depending on the location of the ponds, NaCl, KCl, and traces of gypsum $CaSO_4 \times 2H_2O$ and bischofite ($MgCl_2 \times 6H_2O$).

Sulfate is another impurity to which attention must be paid, since, in excess, it can favor the precipitation of lithium sulfate ($Li_2SO_4 \times H_2O$) in these systems, translating into

yield losses. It must be understood that the sulfate only precipitates a part of the lithium, much of it remaining as lithium chloride.

Brines with higher-than-expected sulfate content are contacted with calcium brine systems, which keeps sulfate levels under control and maintains operations in the chloride field. Under this scenario, the precipitation of gypsum ($CaSO_4 \times 2H_2O$) is favored. A quality indicator of lithium-producing brines corresponds to the SO_4/Ca ratio, which must be maintained at values close to 2.4, which represents the stoichiometric ratio for sulfate and calcium according to their molecular weights.

The harvested salts of potassium carnallite can be leached with water in the stirred reactors, solubilizing a high percentage of the magnesium in the solution. The solids filtered from this process constitute the production of "synthetic" sylvinite [3,4].

4.10. Bischofite Systems

The main objective of bischofite systems ($MgCl_2 \times 6H_2O$) is to concentrate the lithium in the brine. In this stage, the lithium content increases to approximately 4.5% in the brine with a magnesium concentration around 4% [14]. The lithium yield in the bischofite precipitation field can be affected by concepts of impregnation in the crystallized salts; therefore, after harvesting, it is necessary to subject these salts to a drainage process. The drainage stage (also called squeezing) consists of arranging the salts in the form of piles on a slightly inclined surface, which have a waterproof layer at their base, necessary for brine recovery. Drainage or squeezing can be benefited by irrigation of solutions on the pile. Depending on the lithium content in the brine recovered from the squeezes, it is reincorporated into the evaporation process in the ponds with similar concentrations. One part is the bischofite, which is commercialized for its application in the stabilization of roads, as well as in the control of dust and thaw on the same routes.

4.11. Lithium Carnallites

During the lithium concentration process, one of the main impurities is magnesium, which, in excess, in the most concentrated ponds, generates the precipitation of lithium carnallite, and therefore, lithium yield losses. On the other hand, magnesium presents drawbacks in subsequent purification stages, which makes it necessary to remove it to ensure a high-purity lithium carbonate or lithium hydroxide product [37].

In the ponds, a part of the magnesium is separated from the lithium through the precipitation of potassium carnallite, and later as bischofite. However, the separation of lithium and magnesium ions is particularly complex in the most concentrated systems, since they have a very similar ionic size, which makes their chemical behavior similar. It is in this context that the importance of the Mg/Li ratio arises as a parameter for the definition and control of brine transfer and salt precipitation processes. The Salar de Atacama presents a Mg/Li ratio of 6.4 in the lithium-producing ponds, which, in comparison to other deposits, favors an efficient operation in technical and economic terms [38].

In order to reduce the precipitation of lithium carnallite, these brines are contacted with a saturated solution in KCl, which generates the precipitation of potassium carnallite and an decrease in the magnesium content in the concentrated lithium brine. This process can be developed directly in the ponds or in stirred reactors.

Lithium recovery from lithium carnallite salts is possible through leaching with less saturated brine and process water [14]. In this process, the lithium carnallite salts are converted to bischofite, while the lithium is solubilized and reincorporated into the system. SQM has the PC1 Plant that has been used for the agitated leaching of lithium carnallite, achieving yields of around 83% [27].

4.12. Concentrated Brine

By the end of the evaporation process in the ponds of the Salar de Atacama, which takes about 12–18 months, lithium has been concentrated in the brine from 0.15–0.20% to 6%, with magnesium and boron contents of 1.4% and 0.8% respectively [14], in addition to

lower concentrations of calcium, sulfate, potassium, and sodium (see Table 7). This brine is disposed of in the lithium reservoirs, which fulfill the function of finally concentrating the lithium-rich brine and serve as storage to later be transported via tanker trucks to the lithium carbonate and lithium hydroxide plant in Salar del Carmen [27].

Table 7. Chemical composition of the high boron lithium concentrated brine (modified from: [4]).

Li	Mg	Na	K	Ca	SO_4	B	Cl
6.00%	1.40%	0.08%	0.02%	0.033%	0.019%	0.80%	35%

4.13. Harvest and Impregnation

The crystallization process in the ponds generates a continuous growth of salts [39], increasing the floor level of the ponds, and thereby, a decrease in the volume available for the disposal of the brine. The maximum height of precipitation can be defined by different operational criteria and must be controlled periodically through geo-measurements.

In the case of halites, the maximum height of the precipitated salts will be limited by the design height that ensures the necessary residence time for the brine in the concentration process. Once this maximum operational height is reached, the halite salts must be extracted from the pond and transferred to the salt disposal stockpiles, in a process called "salt harvesting" (see Figure 12) [39].

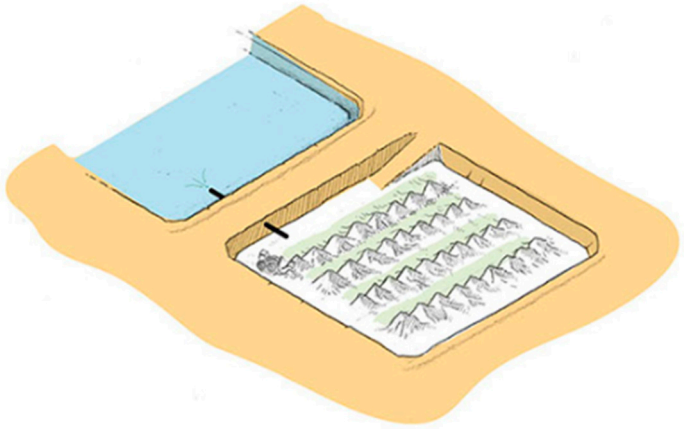

Figure 12. Cordoning process of precipitated salts.

Prior to harvest, and to ensure minimal yield losses due to impregnation, the salts undergo a natural drainage process, which is supported in the first instance with the construction of channels or trenches to facilitate drainage and direct the brine toward strategic accumulation points, such as pumps or sumps; the latter being a deeper suction point for brine transfer to neighboring ponds. The recovered brine is transferred to the operational ponds that follow them in the agreement process.

A second drainage process is affected through the displacement and arrangement of the salts in the form of laces. This cordoning process favors a greater recovery of impregnated brine, as well as a greater area of exposure to solar radiation and with it a reduction in the moisture content prior to harvest. The residual impregnation levels after drainage will depend on the chemical composition of the salts, the size distribution, and crystal nucleation mechanisms, among other operational factors. The height of the laces will depend on the magnitude of the crystallized salts during the operation of the pond.

Once the drainage and drying stages in laces are finished, the sampling and characterization of the salts are carried out in accordance with strict quality protocols. With this information, the salts are extracted from the pond and transferred to different destinations according to their chemical composition [4]. In SQM's operations, about 14 million m^3 of

salts are harvested per year, which is equivalent to 35,000–40,000 m^3 of salts per day (see Figure 13).

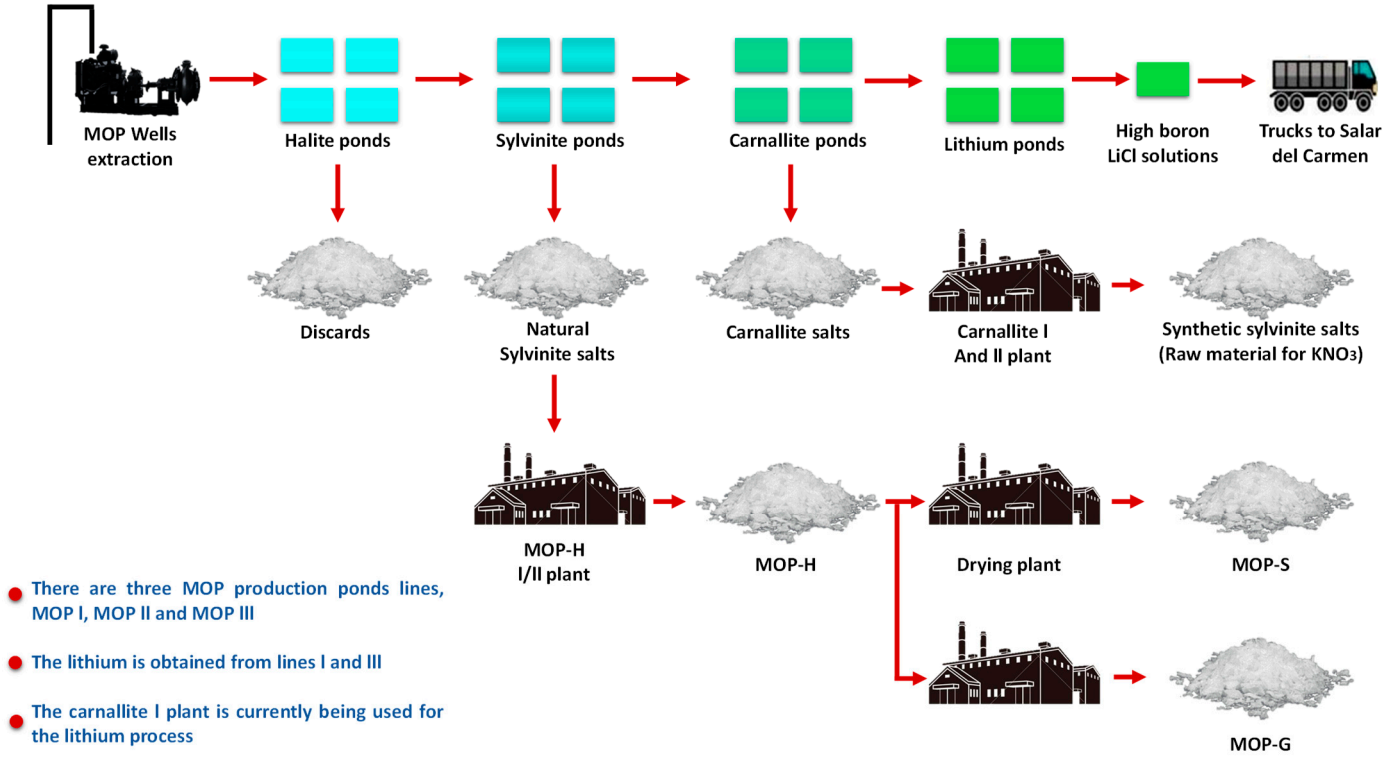

Figure 13. SQM Salar de Atacama production process.

4.14. Salar del Carmen Chemical Plant

The concentrated lithium brine with high boron content from the Salar de Atacama is processed at the Salar del Carmen Plant, located approximately 25 km east of the city of Antofagasta (see Figure 14).

Figure 14. Salar del Carmen, SQM (modified from: [4]).

This brine, which has been transported in tanker trucks, is disposed of in storage ponds. Figure 15 represents a summary of the process that begins with the boron removal stage, where a low boron lithium solution is produced, which could eventually be ready for commercialization. This low boron solution is also the raw material for the lithium carbonate plant. Lithium carbonate can be directly for sale or a part is processed for the production of lithium hydroxide.

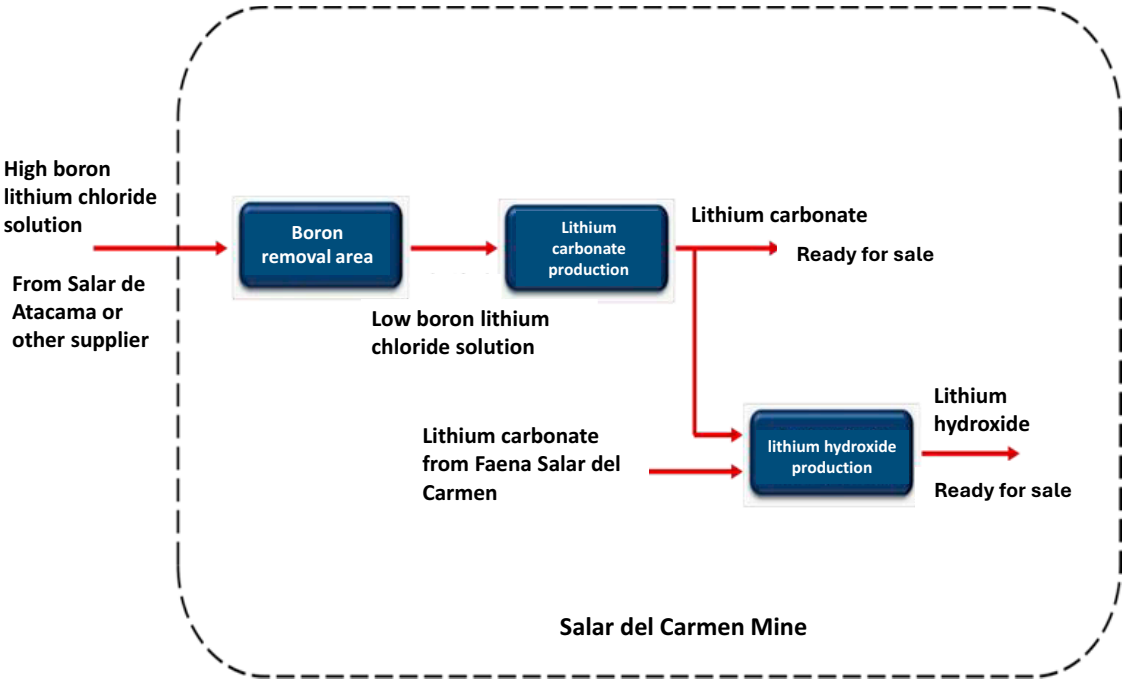

Figure 15. Flow diagram of the Salar del Carmen site.

4.15. Boron Removal

Even though boron has wide industrial applications [40], it has negative effects on lithium production from brines. For example, for the production of aluminum by electrolysis of molten salts, lithium carbonate is used. High boron content in lithium carbonate causes impurities to accumulate in the electrolytic cell until a short circuit is generated. A similar effect occurs in the production of metallic lithium by molten salt electrolysis. In this process, the boron impurities present in lithium chloride purified from lithium carbonate accumulate in the LiCl-KCl electrolyte, producing low efficiency in the electrolytic cells [41].

In the first instance, the concentrated lithium brine with a high boron content (around 8000 ppm) undergoes an acidification process; after which, the residual boron contained in the solution is subjected to a solvent extraction process. In this process, boron is selectively extracted by ion exchange between the aqueous phase and the organic reagent; thus, lithium remains in the concentrated aqueous phase, while boron is transferred to the organic phase as boric acid [14]. The purified lithium solution has reduced the boron contents to less than 30 ppm. It is subsequently filtered and sent to the second stage of magnesium and calcium elimination.

Solvent extraction is a reversible ion exchange process in which the direction of the reaction is controlled by the acidity or pH of the aqueous phase. This principle makes it possible to recover the boron contained in the organic phase through contact with a solution in an alkaline phase in the so-called re-extraction process. In this way, the loaded organic solvent is regenerated and reused in the process, while the boron is transferred to the aqueous phase, which now constitutes a boron-rich liquid industrial waste that is finally sent to the discard ponds. In order to increase the contact between the two phases and improve the transfer of boron, both the extraction and the re-extraction are configured in more than one contact stage of the aqueous and organic phases.

The conventional equipment used in the solvent extraction process corresponds to mixer-settler units, where both phases (organic and aqueous) come into contact in a countercurrent for the time necessary to carry out the exchange. The extraction and separation are achieved mainly based on the difference in density of two immiscible phases [42].

4.16. Purification

The low-boron brine must undergo a two-stage purification process in order to remove the magnesium and calcium present in the solution.

4.16.1. First Phase of Purification

In the first stage of purification, the high magnesium lithium brine is brought into contact with a soda ash solution in stirred reactors. The soda ash solution is previously prepared in a reactor, where the soda ash solid is contacted with the solvent. This soda ash solution is pumped and transported through pipelines to the first-stage purification reactor.

Magnesium carbonate is very sparingly soluble; therefore, this reaction allows most of the magnesium to be broken down as magnesium carbonate, leaving the sodium chloride in solution.

$$MgCl_{2(ac)} + Na_2CO_{3(ac)} \rightarrow MgCO_{3(s)} + 2NaCl_{(ac)} \quad (5)$$

The recovery of the resulting solution reduced in magnesium is carried out through a solid–liquid separation process that uses decanters and later filtration. This purified lithium chloride solution is stored in an accumulation tank, from where it is transported to the next purification stage.

The pulp rich in magnesium carbonate is directed to the sludge treatment area, where it precedes the solid–liquid separation through centrifuges. From this stage, the liquid and solid wastes are obtained, which are transferred to the discard ponds through pumps and trucks, respectively.

4.16.2. Second Phase of Purification

The chloride solution, already reduced in boron and magnesium, goes to a second stage of purification with the aim of reducing the calcium, the remaining magnesium from the previous stage, as well as a large part of the sulfate content [5] The reaction is carried out in a stirred reactor in the presence of milk of lime and soda ash [43], generating magnesium hydroxide and calcium carbonate as products. To obtain slaked lime, there is a lime plant, which consists of a storage prepared to contain granular or powdered lime, as well as an emission control system through bag filters. The reactions of the second purification phase are presented below:

$$Mg^{2+} + Ca(OH)_2 \rightarrow Mg(OH)_{2(s)} + Ca^{2+} \quad (6)$$

$$Mg^{2+} + SO_4^{2-} + Ca(OH)_2 \rightarrow Mg(OH)_{2(s)} + CaSO_{4(s)} \quad (7)$$

$$Ca^{2+} + Na_2CO_3 \rightarrow CaCO_{3(s)} + 2Na^{+} \quad (8)$$

The resulting pulp is sent to clarification equipment, where, through press filters, it is possible to separate the solids (magnesium hydroxide and calcium carbonate) from the clarified lithium solution. The latter is sent to accumulation ponds, where it is directed to the third and final stage. The solids waste produced from the solid–liquid separation are sent to the mud treatment stage described in the first purification phase, to later be transported by truck to the discard ponds.

4.17. Carbonation

The carbonation stage consists of generating the lithium carbonate precipitation reaction from the clarified solution of the previous phase, which previously had to be heated to temperatures normally between 60 and 90 °C [14], and a soda ash solution. This reaction occurs in a series circuit of reactors where mixing occurs. Due to its low solubility, lithium carbonate almost entirely precipitates. On the other hand, due to its inverse solubility, it is possible to increase crystallization with increasing temperature.

The precipitation reaction is described below:

$$2LiCl_{2(ac)} + Na_2CO_{3(ac)} \rightarrow 2NaCl_{(ac)} + Li_2CO_{3(s)} \quad (9)$$

The discharge from the reactors is sent to a hydrocyclone cluster, from where the overflow feeds the decanter of the carbonation stage. The purpose of the decanter of the carbonation stage is to recover the mother liquor from the crystallization stage, as well as the remaining solids from the process.

The underflow of the hydrocyclones feeds the belt filters, from where the pulp is filtered hot and then extensively washed with dematerialized hot water in the filter [44], obtaining the wet lithium carbonate cake, while the filtered brine joins the overflow of the hydrocyclones in the decanter of the carbonation stage. The overflow from the decanter is directed to a filter press where the remaining solid generated in the crystallizer is recovered.

4.18. Dried and Compacted

The drying of the wet lithium carbonate cake is carried out in a rotary dryer equipped with a natural gas and alternative fuel (natural gas) combustion chamber. The dry product is sent to the compaction area. The particulate matter generated in this process is controlled through bag filter systems.

4.19. Packaging Area

The dry product is subjected to a compaction process and later broken up in a hammer mill. Eventually the lithium carbonate can go through a granulation process according to the particle size commitments that are made with the clients. The product is mainly marketed in the form of granules with a minimum purity of 99.2%, with a battery grade of 99.5% [4].

The finished product is classified in vibrating screens and stored in hoppers. The hoppers feed the packaging machine system, where the lithium carbonate is packed in bags, drums, or maxi bags depending on the format available for sale. As in the drying stage, the particulate material is controlled by magic collectors, which direct this material through screw feeders back to the production line (see Figure 16).

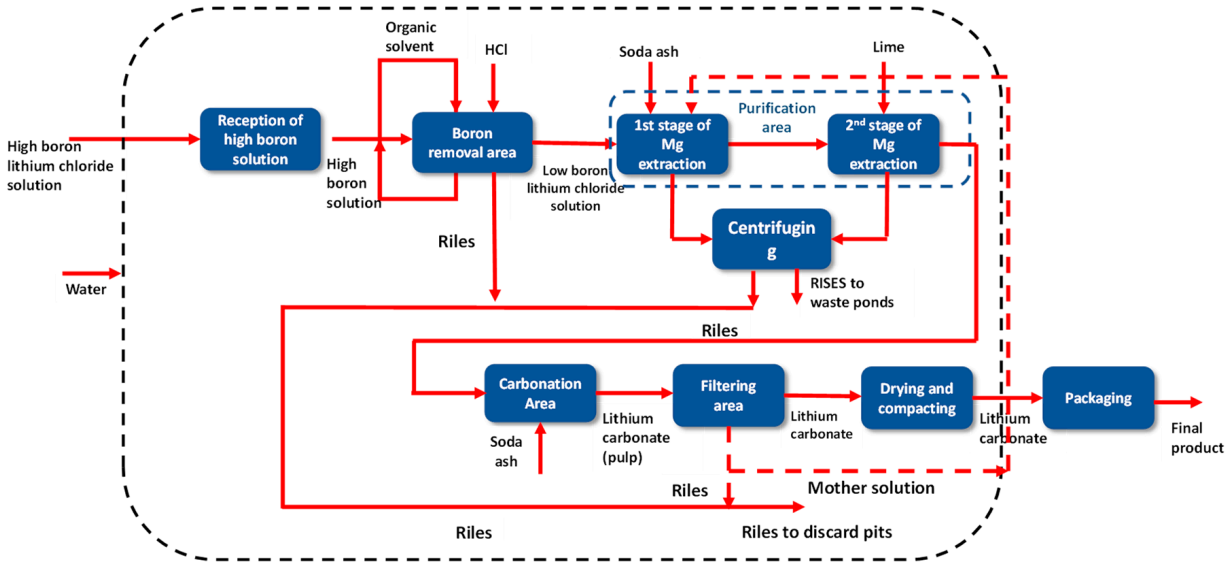

Figure 16. Block diagram of the SQM Salar del Carmen Lithium Carbonate Plant.

4.20. Lithium Hydroxide Plant

Lithium hydroxide production uses lithium carbonate as the main raw material [45,46]. This process has several stages, among the most important are as follows:

- Reaction;
- Clarification and filtration;
- Decantation and centrifugation;

- Evaporation and Crystallization;
- Centrifugation;
- Drying and cooling;
- Packaging and storage.

4.21. Reaction

In this process, the lithium carbonate pulp is pumped and transported through pipes to a series circuit of reactors, where the pulp is contacted with a slaked lime solution [47], generating a metastasis reaction that produces lithium hydroxide in solution and calcium carbonate as a solid. This reaction is endothermic; therefore, heat is required for it to take place [48].

$$Li_2CO_3 + Ca(OH)_2 + 2H_2O \rightarrow 2LiOH \times H_2O + CaCO_3 \quad (10)$$

4.22. Clarification and Filtration

The mixture of dissolved lithium hydroxide and calcium carbonate solids is pumped and conveyed to a clarifier, where solid–liquid separation is achieved with great effectiveness.

On the other hand, the clarified lithium hydroxide solution is filtered to avoid contamination with calcium carbonate that may have been carried over in the clarification process. The result is a solution free of solid residues and ready to enter the evaporation process.

4.23. Decantation and Centrifugation

In order to optimize the yields of the process, the calcium carbonate pulp impregnated with lithium hydroxide is subjected to a backwash process and another solid–liquid separation stage consisting of thickeners, decanters, and centrifuges. Solid calcium carbonate waste with minimal lithium hydroxide content is transported by truck to its final disposal in the solids disposal pond set up for this purpose.

4.24. Evaporation and Crystallization

The conventional method for recovering lithium hydroxide monohydrate is evaporative crystallization. In this process, the clarified and filtered lithium hydroxide solution is transported to a series of evaporators, where sodium hydroxide monohydrate ($LiOH \times H_2O$) crystallizes by evaporating the water present in the solution. It must be taken into account that the solubility of a lithium hydroxide solution is inverse and has an insignificant variation with respect to temperature [46]. The design of crystallization processes is governed by the thermodynamic behavior of the components present (see Figure 17).

Crystallization is a separation method in which the formation of a solid (crystal or precipitate) occurs from a homogeneous, liquid, or gas phase. The evaporation rate is an important parameter in evaporative crystallization. It has been shown that a larger crystal size is achieved with a lower evaporation rate. On the other hand, the higher evaporation rate of the saturated lithium hydroxide solution in turn induces a higher supersaturation rate, resulting in more impure crystals [46,48]. However, crystallization is among the most efficient and accessible methods for obtaining highly purified substances. The geometric arrangement in space of the components of a solid crystal does not allow foreign substances to remain dissolved as impurities. Added to this property and other processing strategies, crystalline lithium hydroxide monohydrate compounds can achieve a high degree of purity.

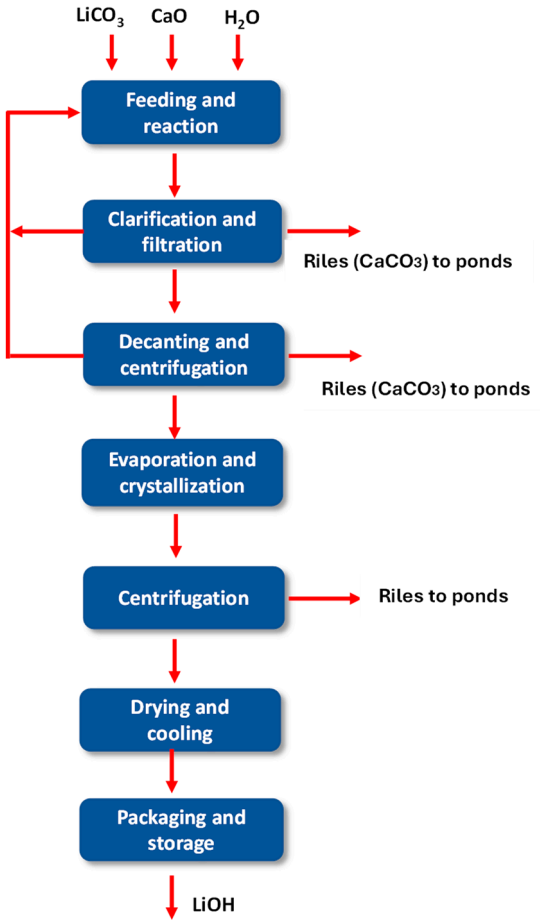

Figure 17. Diagram of the current lithium hydroxide production process.

4.25. Centrifugation

The crystallized monohydrate lithium hydroxide from the previous stage is subjected to a centrifugation process. This operation of separation of the solid particles existing in a suspension by the action of the centrifugal force differs from sedimentation since, in the latter, only the force of gravity acts, so that centrifugation achieves greater effectiveness and in less time of operation.

In this stage of solid–liquid separation, the impurities of chlorides and sulfates that have remained in the system, mainly by mechanical dragging, are eliminated. An important part of the solution resulting from centrifugation is recirculated to the last evaporator, while the rest is purged through pipes to the liquid waste disposal pond, thus avoiding the accumulation of impurities in the lithium hydroxide solution.

4.26. Drying and Cooling

The monohydrated lithium hydroxide crystals maintain residual moisture content from the centrifugation stage. Moisture reduction is accomplished in vibrating fluidized bed drying systems, where material is fed into the dryer from the inlet and continuously advances along with the fluidized bed level under the force of vibration, while hot air passes through from the fluidized bed and exchanges heat with moist lithium hydroxide, becoming humid air. The latter is ejected after passing through the dust collector systems, while the dry material is automatically discharged from the outlet. Subsequently, the material is subjected to a cooling process. This process is carried out in totally encapsulated equipment to avoid any emission that could affect the environment or the product, and under controlled temperature and humidity conditions.

4.27. Packaging and Storage

The monohydrated lithium hydroxide obtained from the drying stage is packaged in bags and/or drums, according to the format and specifications agreed for its sale. The product is stored in the warehouse located next to the plant.

5. Conclusions

Currently, lithium is recovered from brines in the Salar de Atacama through the solar evaporation process, by transferring it in a succession of ponds, where it is possible to go from an initial 0.2% lithium in brines to a 6% concentration of this metal in a period of 18 months, decanting other minerals such as potassium, magnesium, boron, and others.

This process is the most efficient and lowest cost worldwide because the Salar de Atacama has the highest concentrations of lithium in brines in the world with ~1800 ppm, and also high solar radiation that facilitates evaporation (and has no economic cost), and also a good magnesium/lithium ratio that makes the Salar de Atacama more competitive currently than other salt flats in neighboring countries. In addition, this type of process allows the recovery of other minerals such as potassium, which is very important commercially in this type of industry.

Author Contributions: D.T.: writing—original draft, investigation and conceptualization; K.P.: writing—original draft and conceptualization; F.M.G.M.: investigation and writing—review and editing; W.H.L.: investigation and writing—review and editing; E.G.: visualization and validation; E.S.-R.: validation and resources; S.G.: validation and resources; I.J.: visualization and validation; J.C.: visualization and validation; M.S.: conceptualization and resources; N.T.: writing—original draft, supervision and project administration. All authors have read and agreed to the published version of the manuscript.

Funding: This research received no external funding.

Data Availability Statement: The raw data supporting the conclusions of this article will be made available by the authors on request.

Conflicts of Interest: The authors declare no conflict of interest.

References

1. Murodjon, S.; Yu, X.; Li, M.; Duo, J.; Deng, T. Lithium Recovery from Brines Including Seawater, Salt Lake Brine, Underground Water and Geothermal Water. In *Thermodynamics and Energy Engineering*; IntechOpen: London, UK, 2020.
2. Retamal, J.I.; Robles, P.A.; Quezada, G.R.; Jeldres, R.I. Molecular Design and Spodumene Flotation—A Review. *Int. J. Mol. Sci.* **2024**, *25*, 3227. [CrossRef] [PubMed]
3. Morales, Y.; Herrera, N.; Pérez, K. Lithium Carbonate Sedimentation Using Flocculants with Different Ionic Bases. *Hem. Ind.* **2021**, *75*, 205–212. [CrossRef]
4. Toro Villarroel, N.R.; Torres Albornoz, D.A. *La Fuerza Del Litio*; Universidad Arturo Prat: Iquique, Chile, 2023; ISBN 9789564164717.
5. Garrett, D.E. *Handbook of Lithium and Natural Calcium Chloride*; Elsevier: Amsterdam, The Netherlands, 2004; ISBN 9780122761522.
6. Meng, F.; McNeice, J.; Zadeh, S.S.; Ghahreman, A. Review of Lithium Production and Recovery from Minerals, Brines, and Lithium-Ion Batteries. *Miner. Process. Extr. Metall. Rev.* **2021**, *42*, 123–141. [CrossRef]
7. Talens Peiró, L.; Villalba Méndez, G.; Ayres, R.U. Lithium: Sources, Production, Uses, and Recovery Outlook. *JOM* **2013**, *65*, 986–996. [CrossRef]
8. Haynes, W.M. (Ed.) *CRC Handbook of Chemistry and Physics*, 95th ed.; CRC Press: Boca Raton, FL, USA, 2014; ISBN 9780429170195.
9. Seidell, A.; Linke, W.F. Solubilities of Inorganic and Organic Componds. A Compilation of Quantitative Solubility Data from the Periodical Literature. *J. Am. Med. Assoc.* **1928**, *91*, 1131. [CrossRef]
10. Virolainen, S.; Fallah Fini, M.; Miettinen, V.; Laitinen, A.; Haapalainen, M.; Sainio, T. Removal of Calcium and Magnesium from Lithium Brine Concentrate via Continuous Counter-Current Solvent Extraction. *Hydrometallurgy* **2016**, *162*, 9–15. [CrossRef]
11. Housecroft, C.; Sharp, A.G. *Química Inorgánica*; Oxford University Press: Oxford, UK, 2006; ISBN 978-8420548470.
12. Rochow, E.G. *Química Inorgánica*; Oxford University Press: Oxford, UK, 2008; ISBN 978-8429174847.
13. Gray, H.B. *Chemical Bonds: An Introduction to Atomic and Molecular Structure*; University Science Books: Sausalito, CA, USA, 1994; ISBN 978-0935702354.
14. Ehren, P. Process for Producing Lithium Carbonate from Concentrated Lithium Brine. U.S. Patent 2014/0334997 A1, 13 November 2014.
15. Boryta, D.A.; Kullberg, T.F.; Thurston, A.M. Revovery of Lithium Componds from Brines. U.S. Patent 6,207,126 B1, 27 March 2001.

16. Perez, W.; Bravo, H.A.C.B.; Suarez, C.; Bravo, M. Method for the Production of Battery Grade Lithium Carbonate from Natural and Industrial Brines. U.S. Patent 8,691,169 B2, 8 April 2014.
17. Hamzaoui, A.H.; M'nif, A.; Hammi, H.; Rokbani, R. Contribution to the Lithium Recovery from Brine. *Desalination* **2003**, *158*, 221–224. [CrossRef]
18. Intaranont, N.; Garcia-Araez, N.; Hector, A.L.; Milton, J.A.; Owen, J.R. Selective Lithium Extraction from Brines by Chemical Reaction with Battery Materials. *J. Mater. Chem. A* **2014**, *2*, 6374–6377. [CrossRef]
19. Godfrey, L.; Álvarez-Amado, F. Volcanic and Saline Lithium Inputs to the Salar de Atacama. *Minerals* **2020**, *10*, 201. [CrossRef]
20. Fukuda, H. Lithium Extraction from Brine with Ion Exchange Resin and Ferric Phosphate. Ph.D. Thesis, University of British Columbia, Vancouver, BC, Canada, 2019.
21. García-Gil, A.; Vázquez-Suñé, E.; Ayora, C.; Tore, C.; Henríquez, Á.; Yáñez, J. Impacts of the Transient Skin Effect during Brine Extraction Operations in a Crystalline Halite Aquifer. *J. Hydrol.* **2019**, *577*, 123912. [CrossRef]
22. Reutter, K.-J.; Charrier, R.; Götze, H.-J.; Schurr, B.; Wigger, P.; Scheuber, E.; Giese, P.; Reuther, C.-D.; Schmidt, S.; Rietbrock, A.; et al. The Salar de Atacama Basin: A Subsiding Block within the Western Edge of the Altiplano-Puna Plateau. In *Frontiers in Earth Sciences*; Springer: Berlin/Heidelberg, Germany, 2006; pp. 303–325.
23. Muñoz-Pardo, J.F.; Ortiz-Astete, C.A.; Mardones-Pérez, L.; de Vidts-Sabelle, P. Funcionamiento Hidrogeológico Del Acuífero Del Núcleo Del Salar de Atacama, Chile. *Ing. Hidraul. Mex.* **2004**, *19*, 69–81.
24. Lovera, J.A.; Graber, T.A.; Galleguillos, H.R. Correlation of Solubilities for the NaCl + LiCl + H_2O System with the Pitzer Model at 15, 25, 50, and 100 °C. *Calphad* **2009**, *33*, 388–392. [CrossRef]
25. Munk, L.A.; Boutt, D.F.; Hynek, S.; Moran, B. Hydrogeochemical Fluxes and Processes Contributing to the Formation of Lithium-Enriched Brines in a Hyper-Arid Continental Basin. *Chem. Geol.* **2018**, *493*, 37–57. [CrossRef]
26. Marazuela, M.A.; Vázquez-Suñé, E.; Custodio, E.; Palma, T.; García-Gil, A.; Ayora, C. 3D Mapping, Hydrodynamics and Modelling of the Freshwater-Brine Mixing Zone in Salt Flats Similar to the Salar de Atacama (Chile). *J. Hydrol.* **2018**, *561*, 223–235. [CrossRef]
27. Yañez, O. Gestión del Conocimiento en Sqm Salar. Master's Thesis, Universidad de Chile, Santiago, Chile, 2006.
28. Lagos, G. *El Desarrollo Del Litio En Chile: 1984–2012*; Centro de Minerí: Santaigo, Chile, 2012. Available online: http://www.gustavolagos.cl/uploads/1/2/4/2/12428079/el_desarrollo_del_litio_en_chile_g._lagos_21-8-12_a.pdf (accessed on 15 September 2024).
29. Jordan, T.E.; Muñoz, N.; Hein, M.; Lowenstein, T.; Godfrey, L.; Yu, J. Active Faulting and Folding without Topographic Expression in an Evaporite Basin, Chile. *Geol. Soc. Am. Bull.* **2002**, *114*, 1406–1421. [CrossRef]
30. Marazuela, M.A.; Ayora, C.; Vázquez-Suñé, E.; Olivella, S.; García-Gil, A. Hydrogeological Constraints for the Genesis of the Extreme Lithium Enrichment in the Salar de Atacama (NE Chile): A Thermohaline Flow Modelling Approach. *Sci. Total Environ.* **2020**, *739*, 139959. [CrossRef]
31. Amado, F.A.; Rosales, M.; Cofré, E.; Godfrey, L. Sources of Lithium in Brine Deposits of the Atacama Desert, Northern Chile. In Proceedings of the Goldschmidt Conference, Barcelona, Spain, 18–23 August 2019; p. 73.
32. Munk, L.A.; Hynek, S.A.; Bradley, D.C.; Boutt, D.; Labay, K.; Jochens, H. Lithium Brines: A Global Perspective. In *Rare Earth and Critical Elements in Ore Deposits*; Society of Economic Geologists: Littleton, CO, USA, 2016; pp. 1–9.
33. Heidari, N.; Momeni, P. Selective Adsorption of Lithium Ions from Urmia Lake onto Aluminum Hydroxide. *Environ. Earth Sci.* **2017**, *76*, 551. [CrossRef]
34. Collazo, S. Evaporación Mecánica de Salmueras de Litio. Diploma Thesis, Universidad Andrés Bello, Santiago, Chile, 2017.
35. Igsa Consultores. *Cambios y Mejoras de La Operación Minera En El Salar de Atacama*; Igsa Consultores: Santiago, Chile, 2005.
36. da Silva, R.G.; Seckler, M.; Rocha, S.D.F.; Saturnino, D.; de Oliveira, É.D. Thermodynamic Modeling of Phases Equilibrium in Aqueous Systems to Recover Potassium Chloride from Natural Brines. *J. Mater. Res. Technol.* **2017**, *6*, 57–64. [CrossRef]
37. An, J.W.; Kang, D.J.; Tran, K.T.; Kim, M.J.; Lim, T.; Tran, T. Recovery of Lithium from Uyuni Salar Brine. *Hydrometallurgy* **2012**, *117–118*, 64–70. [CrossRef]
38. Yaksic, A.; Tilton, J.E. Using the Cumulative Availability Curve to Assess the Threat of Mineral Depletion: The Case of Lithium. *Resour. Policy* **2009**, *34*, 185–194. [CrossRef]
39. Soto-Bubert, A.; de las Pozas, C.; Navarro, G.; Acevedo, R. *Drenaje de Salmueras En Sales de Halita*; Universidad Mayor: Santiago, Chile, 2019.
40. Fan, X.; Yu, X.; Guo, Y.; Deng, T. Recovery of Boron from Underground Brine by Continuous Centrifugal Extraction with 2-Ethyl-1,3-Hexanediol (EHD) and Its Mechanism. *J. Chem.* **2018**, *2018*, 7530837. [CrossRef]
41. Wilkomirsky, I. Process for Removing Boron from Brines. U.S. Patent 5,939,03, 7 August 1999.
42. Martin, S.L.D.; Díaz, N.G.; Frades, T.M. Mixing and Settling Method and Device in Solvent Extraction Processes to Recover High-Purity Products. U.S. Patent 2005/021 A1, 6 October 2005.
43. Cabrera, V.; Velásquez, C. Factibilidad Tecnico Economica de La Producción de Hidróxido de Litio a Pequeña Escala a Partir de Salmueras. In Proceedings of the 17th LACCEI International Multi-Conference for Engineering, Education, and Technology: "Industry, Innovation, and Infrastructure for Sustainable Cities and Communities", Montego Bay, Jamaica, 24–26 July 2019; Latin American and Caribbean Consortium of Engineering Institutions: Boca Raton, FL, USA, 2019.
44. Grágeda, M.; González, A.; Alavia, W.; Ushak, S. Development and Optimization of a Modified Process for Producing the Battery Grade LiOH: Optimization of Energy and Water Consumption. *Energy* **2015**, *89*, 667–677. [CrossRef]

45. Taboada, M.E.; Graber, T.A.; Cisternas, L.A.; Cheng, Y.S.; Ng, K.M. Process Design for Drowning-Out Crystallization of Lithium Hydroxide Monohydrate. *Chem. Eng. Res. Des.* **2007**, *85*, 1325–1330. [CrossRef]
46. Graber, T.A.; Taboada, M.E.; Cortés, L.; Piceros, E.; Meruane, G.; Aguilar, P. Reactive Crystallization Process of Li2CO3 from LiCl and Na2CO3 Mechanism and Modeling. *Ind. Eng. Chem. Res.* **2024**, *63*, 10299–10308. [CrossRef]
47. Graber, T.A.; Morales, J.W.; Robles, P.A.; Galleguillos, H.R.; Taboada, M.E. Behavior of $LiOH{\cdot}H_2O$ Crystals Obtained by Evaporation and by Drowning Out. *Cryst. Res. Technol.* **2008**, *43*, 616–625. [CrossRef]
48. Kim, K. Recovery of Lithium Hydroxide from Spent Lithium Carbonate Using Crystallizations. *Sep. Sci. Technol.* **2008**, *43*, 420–430. [CrossRef]